Progress In Electromagnetics Research M, Vol. 53, 111–120, 2017

Analogy between Circular Core-Cladding and Impedance Waveguides and Their Membrane Functions

Vitalii I. Shcherbinin[1, *], Gennadiy I. Zaginaylov[1, 2], and Viktor I. Tkachenko[1, 2]

Abstract—One-side boundary conditions on the field inside core region are obtained for core-cladding waveguide with anisotropic cladding. The boundary conditions involve two functions acting as components of anisotropic surface impedance for cladding material. These functions are determined in relation to desired values for step-index waveguide and dielectric-lined waveguide with either perfectly or finitely conducting walls. With resulting surface impedance, the perfect analogy between core-cladding and impedance waveguide is achieved. Using this analogy, independent eigenvalue problems are obtained for membrane functions of HE and EH waves of core-cladding waveguide. From this result some conclusions about electromagnetic properties of HE and EH waves are drawn.

1. INTRODUCTION

Dielectric waveguides [1] are widely used in various branches of modern science and technology. Among other applications, dielectric-loaded waveguides have found applications in gyro-devices including gyrotron [2–4], gyro-TWT [5–13], CARM [14] and others [15–29]. The gyro-devices usually employ RF structures with small structural nonuniformities. Such structures support electromagnetic modes, which have much the same transverse field pattern as eigenmodes of conventional uniform waveguide. For this reason, solutions to eigenvalue problem for uniform waveguide form the basis of gyrotron theory. They are also the subject of our investigation.

Most of the above-listed studies devoted to the dielectric-loaded gyro-devices deal with eigenfields lacking variation along certain direction. For the most widespread guiding structure of circular cross-section such eigenfields correspond to axially-symmetric modes. These modes are pure TE and TM modes. Except for them, the eigenmodes of dielectric-loaded circular waveguide are hybrid HE and EH modes.

It is well known that the field of TE or TM wave is expressed in terms of a single scalar function called membrane function. The membrane functions for TE and TM waves are uncoupled and satisfy independent eigenvalue problems. Contrary to this, the field of any hybrid wave of dielectric-loaded waveguide is expressed in terms of two scalar functions coupled by either or both the continuity and the boundary conditions on the field. Therefore, usually it is impossible to deal with each type of hybrid waves separately. This makes the waveguide problem for hybrid waves more complicated as compared to that for TE or TM waves. As a result, HE and EH waves are governed by common dispersion equation. This may sometimes lead to confusion with mode designation for solutions of dispersion equation, especially when their spectrum is rather dense.

A simple way to avoid this problem for a circular waveguide with anisotropic impedance surface was proposed in [30]. It was shown that the field of any hybrid wave in such guide can be expressed in terms of a single membrane function. There are two membrane functions, each relating to either HE or EH

Received 9 November 2016, Accepted 30 December 2016, Scheduled 22 January 2017
* Corresponding author: Vitalii I. Shcherbinin (vshch@ukr.net).
[1] National Science Center "Kharkiv Institute of Physics and Technology", Kharkiv, Ukraine. [2] V. N. Karazin Kharkiv National University, Kharkiv, Ukraine.

waves and satisfying independent eigenvalue problem. In this connection, hybrid waves of impedance guide are somewhat similar to pure TE and TM waves. Solutions to eigenvalue problems for HE or EH waves are independent dispersion equations. Compared to the common dispersion equation (see, for example, [31–33]), these equations are individually much simpler in form, have sparser spectrum of solutions and do not cause any confusion with mode designation. Besides, it was proven that HE and EH waves of impedance waveguide always behave like TE and TM waves, respectively. To our knowledge, there is no other proof of this fact to this day. The above-discussed results provide additional insights into electromagnetic properties of hybrid waves of impedance waveguide. Moreover, separate treatment for HE and EH hybrid waves can be used to alleviate more general and more complicated problem of beam-wave interaction in impedance waveguide, in particular, for guides used in gyro-devices.

Much the same results can be obtained for several core-cladding dielectric waveguides. To show this in our study, we have reduced the required continuity and boundary conditions for core-cladding waveguide to one-side boundary conditions on the field inside the core region. The resultant boundary conditions were found to have the same form as for circular waveguide with anisotropic surface impedance. We have determined the components of effective surface impedance as functions of cladding parameters and desired eigenfrequency for step-index waveguide and perfectly conducting (PEC) waveguide with dielectric-lined surface. In the general case these components appear to be mode-dependent. This differentiates our results from those presented in [34], which are mainly related to several special cases of frequency-dependent surface impedance. Besides, our study differs from [34] in that it concerns anisotropic cladding material [35–37].

2. CIRCULAR DIELECTRIC-LOADED WAVEGUIDE WITH ANISOTROPIC IMPEDANCE SURFACE

As a preliminary, we briefly review the main results [30] for a circular uniform waveguide bounded by anisotropic impedance surface and filled completely with homogeneous isotropic dielectric. The aim is to find solution $\{\mathbf{E},\mathbf{H}\} = A\{\mathbf{e}(r,\phi),\mathbf{h}(r,\phi)\}\exp(-i\omega t + ik_z z)$ to the wave equations

$$\left(\Delta_\perp + k_\perp^2\right) h_z = 0, \quad \left(\Delta_\perp + k_\perp^2\right) e_z = 0 \tag{1}$$

with the following boundary conditions:

$$\left.\frac{e_\phi}{h_z}\right|_{r=R} = \eta_\phi, \left.\frac{h_\phi}{e_z}\right|_{r=R} = -\eta_z^{-1}, \tag{2}$$

where ω and A are the wave frequency and amplitude, respectively; k_z and $k_\perp = \sqrt{\varepsilon k^2 - k_z^2}$ are the axial and the transverse wavenumbers, respectively; k is the wave vector in free space; R is the waveguide radius; ε is the complex permittivity of dielectric; η_z and η_ϕ are the arbitrary wall impedances in axial and azimuth directions, respectively.

We seek solution to Eqs. (1) and (2) in the following form:

$$h_z = h_z(r)\cos(l\phi), \quad e_z = e_z(r)\sin(l\phi), \tag{3}$$

where l is the azimuth wavenumber.

According to Maxwell's equations, the transverse components of the field are expressed in terms of two scalar functions h_z and e_z, as

$$\mathbf{e}_\perp = \frac{i}{k_\perp^2}\left[k\left(\nabla_\perp h_z \times \mathbf{z}\right) + k_z \nabla_\perp e_z\right], \quad \mathbf{h}_\perp = \frac{i}{k_\perp^2}\left[k_z \nabla_\perp h_z - \varepsilon k\left(\nabla_\perp e_z \times \mathbf{z}\right)\right], \tag{4}$$

where $\nabla_\perp$ is the transverse derivative operator.

In view of Eqs. (3) and (4), the boundary conditions in Eq. (2) can be written in the form:

$$\left.\frac{dh_z}{dr} - \frac{ik_\perp^2\eta_\phi}{k}h_z - \frac{lk_z}{kR}e_z\right|_{r=R} = 0, \quad \left.\frac{de_z}{dr} - \frac{ik_\perp^2\eta_z^{-1}}{\varepsilon k}e_z - \frac{lk_z}{\varepsilon kR}h_z\right|_{r=R} = 0. \tag{5}$$

The boundary conditions in Eq. (5) relate the axial field components h_z and e_z, which are both non-zero for hybrid waves. This property differentiates the field of a hybrid wave from that of pure TE ($e_z = 0$) or pure TM ($h_z = 0$) waves. As a result, the waveguide problem for hybrid waves is more

complicated than that for TE or TM waves. For circular impedance waveguide, however, this problem can be greatly simplified.

In this case, solutions $h_z(r)$ and $e_z(r)$ to Equation (1) are both equal to the single membrane function $\psi(r) = J_l(k_\perp r)$ within a constant factor, where $J_l(x)$ is the Bessel function. Therefore, one can write $h_z(r)$ and $e_z(r)$ as

$$h_z = \sqrt{\varepsilon}\psi(r), \quad e_z = P\psi(r), \tag{6}$$

where $P = P(\omega, k_z)$ is the unknown quantity called hybridization parameter. In what follows notation (ω, k_z) is used to emphasize that the quantity depends on both the wave frequency ω and the axial wavenumber k_z, and therefore is mode-dependent.

Using Eq. (6), one can also express the transverse components in Eq. (4) of the field in terms of membrane function $\psi(r)$. In particular,

$$e_\phi = -\frac{i}{k_\perp^2}\left[\sqrt{\varepsilon}k\frac{d\psi}{dr} - k_z P\frac{l}{r}\psi\right]\cos(l\phi), \quad h_\phi = \frac{i\sqrt{\varepsilon}}{k_\perp^2}\left[\sqrt{\varepsilon}kP\frac{d\psi}{dr} - k_z\frac{l}{r}\psi\right]\sin(l\phi). \tag{7}$$

Rewriting the boundary conditions in Eq. (5) in terms of Eq. (6), we obtain Robin boundary condition [38] on $\psi(r)$:

$$\left[\frac{d\psi}{dr} + \lambda(\omega, k_z)\psi\right]_{r=R} = 0, \tag{8}$$

where $\lambda(\omega, k_z) = (a + bP) = (c + bP^{-1})$, $a = -ik_\perp^2\eta_\phi/k$, $c = -ik_\perp^2/(\varepsilon k\eta_z)$, $b = -lk_z/(\sqrt{\varepsilon}kR)$, hybridization parameter P equals P_1 for HE waves or P_2 for EH waves [34],

$$P_{1,2} = \alpha\left(1 \mp \sqrt{1 + \alpha^{-2}}\right) \tag{9}$$

$\alpha = (c - a)/(2b), P_1P_2 = -1$. Thus, we have two independent eigenvalue problems for different membrane functions $\psi(r)$, one for HE waves ($P = P_1$) and another for EH waves ($P = P_2$).

It is evident from Eq. (9) that the hybridization parameter P must be zero for pure TE waves ($e_z/h_z = 0$) and infinity for pure TM waves ($h_z/e_z = 0$). Therefore, hybrid waves satisfying $|P| < 1$ or $|P| > 1$ will be called TE-like or TM-like waves, respectively.

It can be seen from Eq. (6) that the hybridization parameter P for each hybrid wave is the function of a single variable α, which combines the wave characteristics (ω, k_z, l) and the waveguide parameters (R, ε, η_z and η_ϕ). What is more remarkable, it does not depend explicitly on the membrane function $\psi(r)$. From Eq. (9) it follows that $|P_1| \leq 1$ and $|P_2| \geq 1$ for arbitrary value of α. This proves that HE and EH waves of impedance waveguide are generally TE-like and TM-like waves, respectively. The waves transform to pure TE and TM as α tends to infinity. This occurs in each of the following limiting cases: $k_z \to 0$, $\eta_z \to 0$ and $\eta_\phi \to \infty$.

Substitution of $\psi(r) = J_l(k_\perp r)$ into Eq. (8) gives the dispersion equation for either HE or EH waves

$$k_\perp J_l'(k_\perp R) + \lambda(\omega, k_z) J_l(k_\perp R) = 0, \tag{10}$$

depending on value (P_1 or P_2) of hybridization parameter.

Alternatively [39], this equation may be deduced from the general (common) dispersion equation, which yields the axial wavenumbers $k_z(\omega)$ for hybrid modes of both HE and EH types. Compared to the general dispersion equation, Eq. (10) has much simpler form and sparser spectrum of solutions.

Once $k_z = k_{zs}(\omega)$ has been determined for $\mathrm{HE}_{l,s}$ (or $\mathrm{EH}_{l,s}$) mode of impedance waveguide, it becomes a straightforward matter to find the transverse wavenumber $k_{\perp s}(\omega)$, the hybridization parameter $P(\omega, k_{zs})$, the membrane function $\psi_s(r)$, and finally the field $\{\mathbf{e}_s, \mathbf{h}_s\}$ of this mode. In the case of mode-independent impedance components $\eta_z = \eta_z(\omega)$ and $\eta_\phi = \eta_\phi(\omega)$, such modes of both types form an infinite orthogonal set [34, 40, 41], so that

$$A_s^2 \int_0^R r dr \int_0^{2\pi} d\phi \left[\mathbf{e}_s(r, \phi) \times \mathbf{h}_n(r, \phi)\right]_z = N_s\delta_{sn}, \tag{11}$$

where A_s and N_s are the amplitude and the normalization factor for the field of s-th mode, respectively, δ_{sn} is the Kronecker delta.

However, such is not always the case for impedance guides. An illustrative example is the circular PEC waveguide with axially corrugated wall [34, 42, 43]. When the number of periodic corrugations N is large enough ($N > 2l$), field inside the corrugations can be approximated by that of a single axially symmetric TE mode. By averaging the ratios between ϕ and z components of this field over the period $p = 2\pi R/N$ of corrugations, one obtains components of the effective surface impedance

$$\eta_\phi(\omega, k_z) = -i\frac{w}{p}\frac{k}{k_{\perp I}}\tan(k_{\perp I}d), \quad \eta_z = 0 \tag{12}$$

for $|k_{\perp I}R| \gg 1$. Here $k_{\perp I} = \sqrt{\varepsilon_I k^2 - k_z^2}$; ε_I is the permittivity inside the corrugations; w and d are the corrugation width and depth, respectively.

Obviously, such wall impedance is mode-dependent. In this case, the eigenmodes of impedance waveguide are non-orthogonal. Each of these modes with axial wavenumber $k_z = k_{zs}(\omega)$ is orthogonal to modes of another impedance waveguide, having $\eta_\phi(\omega) = \eta_\phi(\omega, k_{zs}(\omega))$ and $\eta_z = 0$. Setting $\eta_\phi = \eta_\phi(\omega, k_{zs}(\omega))$, we imply in fact that the wave inside the waveguide is matched to the single mode of bounded medium. Such single-mode approximation is the distinct feature of the surface-impedance approach and is often the only means for evaluating the effective surface impedance. It is definitely true for uniform impedance waveguide and may serve as a first approximation for RF structures of gyro-devices [44] with small axial nonuniformities. Note also that in the case of gyrotron, $|k_z^2| \ll |\varepsilon_I k^2|$ for operating and main competing modes. Therefore, for these modes k_z in Eq. (12) is sometimes omitted [45] without significant loss in accuracy.

3. CORE-CLADDING WAVEGUIDE

Consider now the case (Fig. 1), when the core region with the permittivity ε and the radius R is embedded in cladding medium. For generality (see also [35–37]), the cladding medium is assumed to be uniaxial anisotropic and described by the permittivity tensor $\bar{\bar{\varepsilon}}_I$ with non-zero components $\varepsilon_{rrI} = \varepsilon_{\phi\phi I} = \varepsilon_I$ and $\varepsilon_{zzI} = \delta_I\varepsilon_I$. In what follows the subscript "I" denotes quantities related to the cladding region and $\{\mathbf{E}_I, \mathbf{H}_I\} = A_I\{\mathbf{e}_I(r,\phi), \mathbf{h}_I(r,\phi)\}\exp(-i\omega t + ik_z z)$.

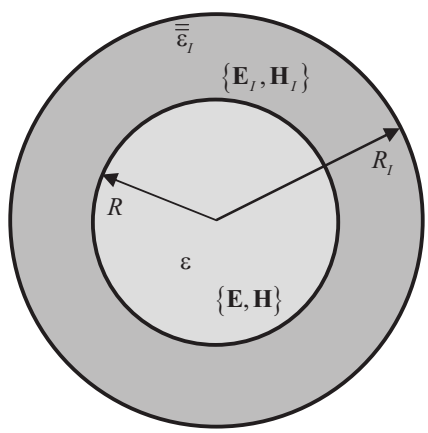

Figure 1. Two-medium model.

Wave field in central dielectric satisfy Eqs. (1), (3) and (4) as before. Meanwhile, the axial and azimuth components of the field must now be continuous at the core-cladding interface. Thus for $r = R$ we have

$$\frac{e_\phi}{h_z} = \frac{e_{\phi I}}{h_{zI}}, \quad \frac{h_\phi}{e_z} = \frac{h_{\phi I}}{e_{zI}}, \quad \frac{e_z}{h_z} = \frac{e_{zI}}{h_{zI}}, \tag{13}$$

where $h_{zI} = h_{zI}(r)\cos(l\phi)$ and $e_{zI} = e_{zI}(r)\sin(l\phi)$.

Note that the transverse and the longitudinal components of the field $\{\mathbf{e}_I, \mathbf{h}_I\}$ in the cladding region are also related by Eq. (4) [35, 36] with ε_I (and $k_{\perp I}$) in place of ε (and $k_\perp$). With this in mind,

we can use Eqs. (3), (4) and (13) to obtain one-side boundary conditions on the field $\{\mathbf{e}, \mathbf{h}\}$ inside the core region

$$\begin{aligned} \left.\frac{dh_z}{dr} - \frac{ik_\perp^2 \eta_{\phi I}}{k} h_z - \frac{lk_z}{kR}\left(1 - \frac{k_\perp^2}{k_{\perp I}^2}\right) e_z\right|_{r=R} &= 0, \\ \left.\frac{de_z}{dr} - \frac{ik_\perp^2 \eta_{zI}^{-1}}{\varepsilon k} e_z - \frac{lk_z}{\varepsilon kR}\left(1 - \frac{k_\perp^2}{k_{\perp I}^2}\right) h_z\right|_{r=R} &= 0, \end{aligned} \tag{14}$$

where

$$\eta_{\phi I}(\omega, k_z) = -\frac{ik}{k_{\perp I}^2 h_{zI}} \left.\frac{dh_{zI}}{dr}\right|_{r=R}, \quad \eta_{zI}^{-1}(\omega, k_z) = -\frac{i\varepsilon_I k}{k_{\perp I}^2 e_{zI}} \left.\frac{de_{zI}}{dr}\right|_{r=R}. \tag{15}$$

A comparison of Eqs. (5) and (14) clearly shows the similarity between boundary conditions for impedance and core-cladding waveguides. These conditions become identical in form, when $|k_\perp^2/k_{\perp I}^2| \ll 1$. In this case, the functions $\eta_{\phi I}(\omega, k_z)$ and $\eta_{zI}(\omega, k_z)$ can be explicitly treated as components of the surface impedance for cladding material. This occurs when either $|k_\perp^2/k_z^2| \ll 1$ or $|\varepsilon/\varepsilon_I| \ll 1$. Each of these conditions yields $k_{\perp I} \approx \sqrt{(\varepsilon_I - \varepsilon)}k$ and, as will be seen below, ensures only a weak mode-dependence for impedance components $\eta_{\phi I}(\omega, k_z)$ and $\eta_{zI}(\omega, k_z)$. The first condition is true for waves far from cutoff and the second one for waveguides with extremely low core/cladding permittivity ratio. Such special cases of mode-independent surface impedance have been considered in [34]. However, they do not cover every possible situation. In particular, these cases are hardly related to the operating conditions of dielectric-loaded gyro-devices.

Axial field components inside the core region can still be written as Eq. (6). With such a field representation, boundary conditions in Eq. (14) yield two values

$$P_{1,2} = \alpha_I \left(1 \mp \sqrt{1 + \alpha_I^{-2}}\right) \tag{16}$$

of hybridization parameter $P(\omega, k_z)$ related to the hybrid waves of core-cladding waveguide. Here $\alpha_I = (c_I - a_I)/(2b_I)$, $a_I = -ik_\perp^2 \eta_{\phi I}/k$, $c_I = -ik_\perp^2 \eta_{zI}^{-1}/(\varepsilon k)$, $b_I = -(1 - k_\perp^2/k_{\perp I}^2) lk_z/(\sqrt{\varepsilon} kR)$.

Using Eq. (16), one may rewrite Eq. (14) in alternative form

$$\begin{aligned} \left.\frac{e_\phi}{h_z}\right|_{r=R} &= \left(\eta_{\phi I}(\omega, k_z) + \frac{ilk_z}{\sqrt{\varepsilon} k_{\perp I}^2 R} P(\omega, k_z)\right) = \eta_\phi(\omega, k_z), \\ \left.\frac{h_\phi}{e_z}\right|_{r=R} &= -\left(\eta_{zI}^{-1}(\omega, k_z) + \frac{i\sqrt{\varepsilon} lk_z}{k_{\perp I}^2 R} P^{-1}(\omega, k_z)\right) = -\eta_z^{-1}(\omega, k_z) \end{aligned} \tag{17}$$

and thereby achieve a perfect analogy between core-cladding and impedance waveguides. Thus, given $\eta_{\phi I}(\omega, k_z)$ and $\eta_{zI}(\omega, k_z)$, it is possible to treat explicitly core-cladding waveguide as a waveguide with anisotropic surface impedance. In the general case such surface impedance is mode-dependent.

It should be emphasized that functions $h_{zI}(r)$ and $e_{zI}(r)$ in Eqs. (15)–(17) are still to be determined. They are solutions of the following equations

$$\left(\Delta_\perp + k_{\perp I}^2\right) h_{zI} = 0, \quad \left(\Delta_\perp + \delta_I k_{\perp I}^2\right) e_{zI} = 0 \tag{18}$$

with unknown integration constants.

There are a few waveguide configurations for which $\eta_{\phi I}(\omega, k_z)$ and $\eta_{zI}^{-1}(\omega, k_z)$ in Eq. (15) are free from such constants. Among them are step-index waveguide and PEC waveguide with dielectric-lined wall.

3.1. Step-Index Circular Waveguide

Consider a cylindrical core embedded in infinite cladding medium ($R_I \to \infty$ in Fig. 1). In this case, solutions for Eq. (18) are as follows:

$$h_{zI} = \sqrt{\varepsilon} H_l^{(1)}(k_{\perp I} r), \quad e_{zI} = P_I H_l^{(1)}\left(\sqrt{\delta_I} k_{\perp I} r\right), \tag{19}$$

where $H_l^{(1)}(x)$ is the Hankel function of the first kind, P_I the unknown constant, and δ_I here is assumed to be real and positive for simplicity. For more details, see [35, 36].

For conducting cladding material ($\mathrm{Im}\varepsilon_I > 0$) the form of Eq. (19) ensures the field decay as r grows to infinity. This suggests that the field is mostly concentrated in the core region when embedded in good conductor ($\mathrm{Im}\varepsilon_I \gg |\mathrm{Re}\varepsilon_I|$). For lossless dielectrics such field decay requires the permittivity ε_I to be less than ε. This condition provides the real frequency range $\varepsilon_I < k_z^2/k^2 < \varepsilon$ for waves propagated ($k_\perp^2 > 0$) in the core region and attenuated ($k_{\perp I}^2 < 0$) in the cladding region.

Substitution of Eq. (19) into Eq. (15) gives:

$$\eta_{\phi I}(\omega, k_z) = -\frac{ik}{k_{\perp I}} \frac{H_l'^{(1)}(k_{\perp I}R)}{H_l^{(1)}(k_{\perp I}R)}, \quad \eta_{zI}^{-1}(\omega, k_z) = -\frac{i\varepsilon_I k\sqrt{\delta_I}}{k_{\perp I}} \frac{H_l'^{(1)}\left(\sqrt{\delta_I}k_{\perp I}R\right)}{H_l^{(1)}\left(\sqrt{\delta_I}k_{\perp I}R\right)}. \tag{20}$$

It is seen that the functions $\eta_{\phi I}(\omega, k_z)$ and $\eta_{zI}^{-1}(\omega, k_z)$ for step-index waveguide depend on given azimuth wavenumber l, radius R, permittivity $\bar{\bar{\varepsilon}}_I$ of cladding material and desired axial wavenumber $k_z(\omega)$. These functions represent the well-known impedance components $\eta_{\phi I} \approx 1/\sqrt{\varepsilon_I}$ and $\eta_{zI} \approx 1/\sqrt{\delta_I \varepsilon_I}$ for cladding surface, when $|k_{\perp I}|R$ far exceeds both unity and $\sqrt{\delta_I}$ (e.g., for cladding with a rather high conductivity). The eigenvalue problem Eqs. (1) and (14) for step-index waveguide, in view of Eq. (20), is clearly defined.

Again, as in the Section 2, we may write its solution in the form of Eq. (6). Then, with a_I, b_I and c_I in place of a, b and c, relations in Eqs. (7)–(10) become valid for step-index waveguide. Note that substitution of Eq. (20) into Eqs. (16) and (17) yields a perfect analogy between step-index and impedance waveguides.

Using this analogy, one can conclude that (a) the field inside the core region of step-index waveguide is expressed in terms of a single scalar membrane function $\psi(r)$; (b) for step-index waveguide there exist two membrane functions, each satisfying independent eigenvalue problem and describing hybrid waves of either HE or EH type; (c) solutions to eigenvalue problems are independent dispersion Equations (10) for HE and EH waves; (d) these dispersion equations, taken separately for each type of hybrid waves, have sparser spectrum of solutions, are easier to analyze and do not cause confusion in mode designation; (e) the hybridization parameter P for each hybrid wave depends on single variable $\alpha_I = \alpha_I(l, \omega, k_z, R, \varepsilon, \eta_{\phi I}, \eta_{zI})$; (f) inside the core region of step-index waveguide hybrid HE and EH waves are always TE-like ($|P| \leq 1$) and TM-like ($|P| \geq 1$) waves, respectively.

We now turn our attention to the cladding region. From Eqs. (13) and (19) we obtain

$$P_I = P\frac{H_l^{(1)}(k_{\perp I}R)}{H_l^{(1)}\left(\sqrt{\delta_I}k_{\perp I}R\right)}. \tag{21}$$

Hence it follows that constant P_I equals hybridization parameter P in the case of isotropic cladding material ($\delta_I = 1$). Therefore, in this case, the conditions $P_I \leq 1$ and $P_I \geq 1$ hold true for HE and EH waves, respectively. Thus, whatever the problem parameters are, HE (EH) waves of isotropic step-index waveguide behave generally like TE (TM) waves in the entire space. Besides, note that $\varepsilon_I \eta_{\phi I} \eta_{zI} = 1$ for such guide.

3.2. Circular Waveguide with Dielectric-Lined PEC Wall

Let us next consider the dielectric core of radius R, which is surrounded by anisotropic dielectric layer (cladding) with the radius R_I of outer surface (Fig. 1). At $r = R_I$ the following boundary conditions

$$\left.\frac{dh_{zI}}{dr} + \gamma_H h_{zI}\right|_{r=R_I} = 0 \quad \left.\frac{de_{zI}}{dr} + \gamma_E^{-1} e_{zI}\right|_{r=R_I} = 0 \tag{22}$$

are imposed. With $\gamma_H = \gamma_E = 0$, the boundary conditions in Eq. (22) imply that the external material ($r > R_I$) is the perfect electric conductor with smooth inner surface. In the case of PEC walls with densely spaced axial corrugations (see Eq. (11)), $\gamma_E = 0$ and $\gamma_H \neq 0$.

Axial components of the field inside anisotropic dielectric layer are now given by

$$h_{zI} = \sqrt{\varepsilon} Z_l^{(1)}(k_{\perp I}r), \quad e_{zI} = P_I Z_l^{(2)}\left(\sqrt{\delta_I}k_{\perp I}r\right) \tag{23}$$

where $Z_l^{(n)}(x) = [J_l(x) - B_I^{(n)} N_l(x)]$, $N_l(x)$ is the Neumann function, P_I the unknown constant, and $B_I^{(1)}$ and $B_I^{(2)}$ must be taken as

$$B_I^{(1)} = \frac{k_{\perp I} J_l'(k_{\perp I} R_I) + \gamma_H J_l(k_{\perp I} R_I)}{k_{\perp I} N_l'(k_{\perp I} R_I) + \gamma_H N_l(k_{\perp I} R_I)}, \quad B_I^{(2)} = \frac{\sqrt{\delta_I} k_{\perp I} J_l'\left(\sqrt{\delta_I} k_{\perp I} R_I\right) + \gamma_E^{-1} J_l\left(\sqrt{\delta_I} k_{\perp I} R_I\right)}{\sqrt{\delta_I} k_{\perp I} N_l'\left(\sqrt{\delta_I} k_{\perp I} R_I\right) + \gamma_E^{-1} N_l\left(\sqrt{\delta_I} k_{\perp I} R_I\right)}$$

to fulfill Eq. (22).

Using Eq. (23), we obtain the functions

$$\eta_{\phi I}(\omega, k_z) = -\frac{ik}{k_{\perp I}} \frac{Z_l'^{(1)}(k_{\perp I} R)}{Z_l^{(1)}(k_{\perp I} R)}, \quad \eta_{zI}^{-1}(\omega, k_z) = -\frac{i\varepsilon_I k \sqrt{\delta_I}}{k_{\perp I}} \frac{Z_l'^{(2)}\left(\sqrt{\delta_I} k_{\perp I} R\right)}{Z_l^{(2)}\left(\sqrt{\delta_I} k_{\perp I} R\right)} \tag{24}$$

involved in boundary conditions in Eq. (14), which are free from any uncertain quantities.

With Eq. (24), we have clearly defined eigenvalue problem in Eqs. (1) and (14) for dielectric-lined PEC waveguide. It is analogous to the eigenvalue problem for step-index waveguide and thus may be solved by the procedure described above in the previous subsection. Hence it follows that conclusions made in this subsection are valid for both step-index and dielectric-lined PEC waveguides.

From Eqs. (13) and (24), we obtain

$$P_I = P \frac{Z_l^{(1)}(k_{\perp I} R)}{Z_l^{(2)}\left(\sqrt{\delta_I} k_{\perp I} R\right)}. \tag{25}$$

Hence, for waveguide with isotropic cladding and hard ($\gamma_E = 0$ and $\gamma_H = \infty$) outer surface $r = R_I$, constants P_I and P appear to be equal to each other. This exemplifies the case when HE (EH) hybrid waves are generally TE- (TM-) like waves throughout the perfect conducting waveguide with dielectric-lined surface.

3.3. Circular Conducting Waveguide with Dielectric-Lined Wall

Obviously, perfect conductivity is the idealization, which fails in some cases of practical interest. Therefore, next we consider conducting waveguide with dielectric-lined surface. In this case, the boundary conditions are as follows:

$$\left.\frac{e_{\phi I}}{h_{zI}}\right|_{r=R_I} = Z_\phi, \quad \left.\frac{h_{\phi I}}{e_{zI}}\right|_{r=R_I} = -Z_z^{-1}, \tag{26}$$

where Z_ϕ and Z_z are the components of surface impedance for external material.

The boundary conditions in Eq. (26) give no way of deducing $\eta_{\phi I}$ and η_{zI}^{-1} in Eq. (15) as functions of cladding parameters and desired axial wavenumber $k_z(\omega)$ only. These functions depend also on additional unknown, denoted as P_{II}. A technique for finding this unknown is described below.

In addition to Eq. (26) we introduce extra condition at $r = R_I$

$$\left.\frac{e_{zI}}{h_{zI}}\right|_{r=R_I} = \frac{P_{II}}{\sqrt{\varepsilon}}. \tag{27}$$

With Eq. (27) the boundary conditions in Eq. (26) are reduced to the following form:

$$\left.\frac{dh_{zI}}{dr} + \gamma_H(P_{II}) h_{zI}\right|_{r=R_I} = 0, \quad \left.\frac{de_{zI}}{dr} + \gamma_E^{-1}(P_{II}) e_{zI}\right|_{r=R_I} = 0, \tag{28}$$

where $\gamma_H(P_{II}) = a_{II} + b_{II} P_{II}$, $\gamma_E^{-1}(P_{II}) = c_{II} + (\varepsilon b_{II})/(\varepsilon_I P_{II})$, $a_{II} = -ik_{\perp I}^2 Z_\phi / k$, $b_{II} = -lk_z/(\sqrt{\varepsilon} k R_I)$, $c_{II} = -ik_{\perp I}^2 Z_z^{-1}/(\varepsilon_I k)$.

It is seen that the boundary conditions in Eq. (28) are identical in form to Eq. (22). Therefore, the eigenvalue problem in Eqs. (1), (13) and (28) can be solved in the same manner as for PEC waveguide with dielectric-lined wall. As a result, we obtain functions $\eta_{\phi I}(P_{II})$ and $\eta_{zI}^{-1}(P_{II})$ (see (24)) and also the values $P_1(P_{II})$ and $P_2(P_{II})$ (see Eq. (16)) of hybridization parameter in relation to the unknown

constant P_{II}. Alternatively, the hybridization parameter is found from Eqs. (13) and (27). We equate these alternative expressions of hybridization parameter and thus obtain

$$P_{1,2}\left(P_{II}\right) = P_{II}\frac{Z_l^{(1)}\left(k_{\perp I}R_I\right)}{Z_l^{(1)}\left(k_{\perp I}R\right)}\frac{Z_l^{(2)}\left(\sqrt{\delta_I}k_{\perp I}R\right)}{Z_l^{(2)}\left(\sqrt{\delta_I}k_{\perp I}R_I\right)}. \tag{29}$$

The resulting relation is complementary to the dispersion Equation (10). Both Eqs. (10) and (29) form a system of transcendental equations in two unknowns $k_z(\omega)$ and P_{II}. Analogous system can be derived in the case of multi-layer dielectric waveguide. In this case, extra condition similar to Eq. (27) should be imposed on the field at the outer boundary of the waveguide.

It is well known [46, 47] that for multi-layer waveguide the straightforward derivation yields dispersion equation in the form of zero determinant of large size matrix. To avoid problems associated with such matrices, the so-called matrix approach was proposed in [46]. Our approach is the alternative. In contrast to the matrix approach, it does not involve any matrix operations (inversion, multiplication, etc.). The weakness of our approach is that it yields a system of transcendental equations. By comparison, in the matrix approach the resultant combined equations are linear algebraic.

4. CONCLUSION

We have demonstrated the close analogy between circular waveguide with anisotropic impedance surface, step-index waveguide and perfectly conducting waveguide with dielectric-lined walls. The common feature is the form of eigenvalue problem, which involves components of anisotropic surface impedance. It has been found that for step-index and dielectric-lined PEC waveguides these components depend solely on cladding parameters and desired eigenfrequency.

Using this analogy, we have shown that (a) the field inside the core region of step-index or dielectric-lined waveguides is expressed in terms of single scalar membrane function; (b) HE and EH hybrid waves of these guides have different membrane functions subject to independent eigenvalue problems; (c) solutions to these problems are independent dispersion equations for HE and EH waves; (d) inside the core region of step-index or dielectric-lined waveguides HE and EH hybrid waves behave generally like TE and TM waves, respectively. These results provide additional insights into electromagnetic properties of hybrid waves of step-index and dielectric-lined waveguides.

Besides, a new approach to eigenvalue problem for conducting waveguide with dielectric-lined walls has been proposed. The approach yields a system of two coupled transcendental equations with desired eigenfrequency as one of two unknowns. The possibility of derivation of analogous system for multi-layer dielectric waveguide has been also discussed.

REFERENCES

1. Yeh, C. and F. I. Shimabukuro, *The Essence of Dielectric Waveguides*, 522, Springer Science+Business Media, LLC, New York, 2008.
2. Chen, X., G. Liu, and C. Tang, "Novel dielectric photonic-band-gap resonant cavity loaded in a gyrotron," *J. Phys. D: Appl. Phys.*, Vol. 43, No. 40, 405101, 2010.
3. Huang, Y. J., K. R. Chu, and M. Thumm, "Self-consistent modeling of terahertz waveguide, and cavity with frequency-dependent conductivity," *Physics of Plasmas*, Vol. 22, No. 1, 013108, 2015.
4. Hong, B. B., L. P. Huang, X. L. Xu, Y. X. Xia, and C. J. Tang, "Hollow core photonic crystal for terahertz gyrotron oscillator," *J. Phys. D: Appl. Phys.*, Vol. 48, No. 4, 045104, 2015.
5. Choe, J. Y., H. S Uhm, and S. Ahn, "Analysis of the wide band gyrotron amplifier in a dielectric loaded waveguide," *Journal of Applied Physics*, Vol. 52, No. 7, 4508–4516, 1981.
6. Uhm, H. S., J. Y. Choe, and S. Ahn, "Theory of gyrotron amplifier in a waveguide with inner dielectric material," *Int. J. Electron.*, Vol. 51, No. 4, 521–532, 1981.
7. Rao, S. J., P. K. Jain, and B. N. Basu, "Broadbanding of a gyro-TWT by dielectric-loading through dispersion shaping," *IEEE Trans. Electron Devices*, Vol. 43, No. 12, 2290–2299, 1996.

8. Leou, K. C., D. B. McDermott, and N. C. Luhmann, "Large-signal characteristics of a wide-band dielectric-loaded gyro-TWT amplifier," *IEEE Trans. Plasma Sci.*, Vol. 24, No. 3, 718–726, 1996.
9. Rao, S. J., R. Jain, and B. N. Basu, "Two-stage dielectric-loading for broadbanding a gyro-TWT," *IEEE Electron Device Letters*, Vol. 17, No. 6, 303–305, 1996.
10. Du, C.-H., Q. Z. Xue, and P.-K. Liu, "Loss-induced modal transition in a dielectric-coated metal cylindrical waveguide for gyro-traveling-wave-tube applications," *IEEE Electron Device Letters*, Vol. 29, No. 11, 1256–1258, 2008.
11. Du, C.-H. and P.-K. Liu, "Linear full-wave-interaction analysis of a gyrotron-traveling-wave-tube amplifier based on a lossy dielectric-lined circuit," *IEEE Trans. Plasma Sci.*, Vol. 38, No. 6, 1219–1226, 2010.
12. Du, C.-H. and P.-K. Liu, "Nonlinear full-wave-interaction analysis of a gyrotron-traveling-wave-tube amplifier based on a lossy dielectric-lined circuit," *Physics of Plasmas*, Vol. 17, No. 3, 033104, 2010.
13. Du, C. H., et al., "Design of a W-band gyro-TWT amplifier with a lossy ceramic-loaded circuit," *IEEE Trans. Electron Devices*, Vol. 60, No. 7, 2388–2394, 2013.
14. Yin, Y.-Z., "The cyclotron autoresonance maser with a large-orbit electron ring in a dielectric-loaded waveguide," *Int. J. Infrared Millimeter Waves*, Vol. 14, No. 8, 1587–1600, 1993.
15. Chu, K. R., A. K. Ganguly, V. L. Granatstein, J. L. Hirshfield, S. Y. Park, and J. M. Baird, "Theory of a slow wave cyclotron amplifier," *Int. J. Electron.*, Vol. 51, No. 4, 493–502, 1981.
16. Lin, A. T., W. W. Chang, and K. R. Chu, "Nonlinear efficiency and bandwidth of a slow wave cyclotron amplifier," *Int. J. Infrared Millimeter Waves*, Vol. 5, No. 4, 427–444, 1984.
17. Freund, H. P. and A. K. Ganguly, "Nonlinear analysis of the Cerenkov maser," *Physics of Fluids B*, Vol. 2, No. 10, 2506–2515, 1990.
18. Ganguly, A. K. and S. Ahn, "Nonlinear theory of the slow-wave cyclotron amplifier," *Phys. Rev. A*, Vol. 42, No. 6, 3544–3554, 1990.
19. Vomvoridis, J. L. and M. A. Hambakis, "Non-linear analysis of the electron cyclotron maser with axial initial electron velocity," *Int. J. Electron.*, Vol. 71, No. 1, 167–190, 1991.
20. Iatrou, C. T. and J. L. Vomvoridis, "Microwave excitation and amplification using cyclotron interaction with an axial electron velocity beam," *Int. J. Electron.*, Vol. 71, No. 3, 493–510, 1991.
21. Vomvoridis, J. L. and C. T. Iatrou, "Linear fluid analysis of the electron cyclotron maser with axial initial electron velocity," *Int. J. Electron.*, Vol. 71, No. 1, 145–165, 1991.
22. Cho, Y.-H., D.-I. Choi, and J.-S. Choi, "Electromagnetic wave amplification of cyclotron Cherenkov maser," *Optics Communications*, Vol. 94, No. 6, 530–536, 1992.
23. Cho, Y.-H., D.-I. Choi, and J.-S. Choi, "Cyclotron Cherenkov maser amplification using the anomalous Doppler effect," *Nuclear Instruments and Methods in Physics Research Section A: Accelerators, Spectrometers, Detectors and Associated Equipment*, Vol. 331, No. 1, 572–576, 1993.
24. Lee, C.-Y., R. Yamashita, and M. Masuzaki, "Linear analysis of cyclotron-cherenkov and cherenkov instabilities in dielectric-loaded coaxial waveguides," *Int. J. Infrared Millimeter Waves*, Vol. 18, No. 2, 519–535, 1997.
25. Zhao, D. and Y. Ding, "Cerenkov and cyclotron Cerenkov instabilities in a dielectric loaded parallel plate waveguide sheet electron beam system," *Physics of Plasmas*, Vol. 18, No. 9, 093107, 2011.
26. Zhao, D. and Y. Ding, "Nonlinear analysis of the dielectric loaded rectangular Cerenkov maser," *Physics of Plasmas*, Vol. 19, No. 2, 024508, 2012.
27. Zhao, D. and Y. Ding, "Simplified nonlinear theory of the dielectric loaded rectangular Cerenkov maser," *Chin. Phys. B*, Vol. 21, No. 9, 094102, 2012.
28. Kong, L.-B., H.-Y. Wang, Z.-L. Hou, H.-B. Jin, and C.-H. Du, "The nonlinear theory of slow-wave electron cyclotron masers with inclusion of the beam velocity spread," *Annals of Physics*, Vol. 339, 588–595, 2013.
29. Khalilzadeh, E., A. Chakhmachi, and B. Maraghechi, "Effect of self-fields on the electron cyclotron maser instability in a dielectric loaded waveguide," *The European Physical Journal D*, Vol. 69, No. 11, 256, 2015.

30. Shcherbinin, V. I., G. I. Zaginaylov, and V. I. Tkachenko, "HE and EH hybrid waves in a circular dielectric waveguide with an anisotropic impedance surface," *Problems of Atomic Science and Technology. Plasma Electronics and New Methods of Acceleration*, Vol. 98, 89–93, 2015.
31. Mohsen, A. and M. Hamid, "Wave propagation in a circular waveguide with an absorbing wall," *Journal of Applied Physics*, Vol. 41, No. 1, 433–434, 1970.
32. Elsherbeni, A. Z., J. Stanier, and M. Hamid, "Eigenvalues of propagating waves in a circular waveguide with an impedance wall," *IEE Proceedings H*, Vol. 135, No. 1, 23–26, 1988.
33. Koivisto, P. K., S. A. Tretyakov, and M. I. Oksanen, "Waveguides filled with general biisotropic media," *Radio Science*, Vol. 28, No. 5, 675–686, 1993.
34. Mahmoud, S. F., *Electromagnetic Waveguides: Theory and Applications*, 77–93, Peregrinus, London, 1991.
35. Zhang, Q., T. Jiang, and Y. Feng, "Slow-light propagation in a cylindrical dielectric waveguide with metamaterial cladding," *J. Phys. D: Appl. Phys.*, Vol. 44, No. 47, 475103, 2011.
36. Atakaramians, S., A. Argyros, S. Fleming, and B. Kuhlmey, "Hollow-core waveguides with uniaxial metamaterial cladding: Modal equations and guidance conditions," *J. Opt. Soc. Am. B*, Vol. 29, No. 9, 2462–2477, 2012.
37. Pollock, J. G. and A. K. Iyer, "Experimental verification of below-cutoff propagation in miniaturized circular waveguides using anisotropic ENNZ metamaterial liners," *IEEE Trans. Microwave Theory Tech.*, Vol. 64, No. 4, 1297–1305, 2016.
38. Olver, P., *Introduction to Partial Differential Equations*, 123, Springer-Verlag, New York, 2014.
39. Miyagi, M. and S. Kawakami, "Design theory of dielectric-coated circular metallic waveguides for infrared transmission," *Journal of Lightwave Technology*, Vol. 2, No. 2, 116–126, 1984.
40. Dragone, C., "Reflection, transmission and mode conversion in a corrugated feed," *The Bell System Technical Journal*, Vol. 56, No. 6, 835–867, 1977.
41. Li, H. and M. Thumm, "Mode coupling in corrugated waveguides with varying wall impedance and diameter change," *Int. J. Electron.*, Vol. 71, No. 5, 827–844, 1991.
42. Li, H., F. Xu, and S. Liu, "Theory of harmonic gyrotron with multiconductors structure," *Int. J. Electron.*, Vol. 65, No. 3, 409–418, 1988.
43. Iatrou, C. T., S. Kern, and A. B. Pavelyev, "Coaxial cavities with corrugated inner conductor for gyrotrons," *IEEE Trans. Microwave Theory Tech.*, Vol. 44, No. 1, 56–64, 1996.
44. Shcherbinin, V. I., "Eigenmodes of a gyrotron cavity with anisotropic impedance surface," *Proc. of 9th International Kharkiv Symposium on Physics and Engineering of Microwaves, Millimeter and Submillimeter Waves*, 1–4, Kharkiv, Ukraine, June 20–24, 2016.
45. Dumbrajs, O. and G. S. Nusinovich, "Coaxial gyrotrons: Past, present and future (review)," *IEEE Trans. Plasma Sci.*, Vol. 32, No. 3, 934–946, 2004.
46. Yeh, C. and G. Lindgren, "Computing the propagation characteristics of radially stratified fibers: An efficient method," *Appl. Opt.*, Vol. 16, No. 2, 483–493, 1977.
47. Chou, R. C. and S. W. Lee, "Modal attenuation in multilayered coated waveguides," *IEEE Trans. Microwave Theory Tech.*, Vol. 36, No. 7, 1167–1176, 1988.